Highly Sensitive Amperometric Cholesterol Biosensor Based on Pt-Incorporated Fullerene-like ZnO Nanospheres

Mashkoor Ahmad,[†] Caofeng Pan,[†] Lin Gan,[†] Zeeshan Nawaz,[‡] and Jing Zhu*[,†]

Beijing National Center for Electron Microscopy, The State Key Laboratory of New Ceramics and Fine Processing, Laboratory of Advanced Material, Department of Material Science and Engineering, Tsinghua University, Beijing 100084, China, and Beijing Key Laboratory for Green Chemical Reaction Engineering & Technology, Department of Chemical Engineering, Tsinghua University, Beijing 100084, China

Received: September 16, 2009

A highly sensitive amperometric biosensor based on Pt-incorporated fullerene-like ZnO hybrid nanospheres has been investigated. Pt−ZnO nanospheres (PtZONS) with diameters in the range 50−200 nm have been successfully synthesized by electrodeposition on a glassy carbon electrode (GCE). The Pt nanoparticles in ZnO nanospheres have been identified with high-resolution transmission electron microscopy (HRTEM) and energy dispersive X-ray spectroscopy (EDS). The doped Pt nanoparticles demonstrate the abilities to electrocatalyze the oxidation of hydrogen peroxide and substantially raise the response current. The sensitivity of the PtZONS/GCE to hydrogen peroxide is 147.8 μA μM^{-1} cm^{-2}, which is much higher than that of a conventional electrode. The PtZONS/GCE was functionalized with cholesterol oxidase (ChOx) by physical adsorption. The enzyme electrode exhibits a very high and reproducible sensitivity of 1886.4 mA M^{-1} cm^{-2} to cholesterol with a response time less than 5 s and a linear range from 0.5 to 15 μM. Furthermore, it has been revealed that the biosensor exhibits a good anti-interference ability and favorable stability over relatively long-term storage (more than 5 weeks). All these results strongly suggest that the PtZONS not only enhance the sensitivity to cholesterol but also help to eliminate the interference at low applied potential.

I. Introduction

The development of a cholesterol biosensor is important due to the prevalence of cardiovascular diseases as a major health threat around the world.[1] The concentration of cholesterol in blood is an important parameter for the diagnosis and prevention of disease. Ideally, the total cholesterol concentration in a healthy person's blood should be less than 200 mg/dL (<5.17 mM). The borderline value is defined as 200−239 mg/dL (5.17−6.18 mM), and the high value is defined as above 240 mg/dL (≥6.21 mM).[2] The measurement of blood cholesterol concentration is a routine practice in medical screening or diagnosis. Therefore, a simple and practical highly sensitive cholesterol biosensor is desirable and can be useful in the prevention and the management of cardiovascular disease.

Currently, the development of various cholesterol biosensors represents a very active area in biosensor research. The amperometric biosensor is chosen for biochemical analysis because of its good selectivity, rapid response, and low cost.[3,4] The enzymatic reactions in the use of cholesterol oxidase (ChOx) as a receptor can be described as follows:

$$\text{cholesterol} + O_2 \xrightarrow{\text{ChOx}} \text{cholest-4-en-3-one} + H_2O_2 \quad (1)$$

$$H_2O_2 \xrightarrow{E} O_2 + 2H^+ + 2e^- \quad (2)$$

The cholesterol is catalyzed by ChOx in the presence of oxygen, and as a result hydrogen peroxide is produced at the same time. The electrooxidation current of hydrogen peroxide is detected after application of a suitable potential to the system. The major problem for amperometric detection is the overestimation of the response current due to interferences. Recently, many researchers have reported the inclusion of metal nanoparticles with a catalytic effect in polymer modified electrodes to improve biosensor sensibility and to decrease the overpotential applied to the amperometric biosensors.[5−11] Pt is a well-known catalyst that has a high catalytic activity for hydrogen peroxide electrooxidation.[12−14]

Nanomaterials provide high surface areas for higher enzyme loading and a compatible microenvironment helping the enzyme to retain its bioactivity. Besides this, they provide direct electron transfer between the enzyme's active site and the electrode.[15−18] Among the nanomaterials, zinc oxide (ZnO), a wide band gap semiconductor, has attracted much attention due to its wide range of applications.[19−22] ZnO nanostructures exhibit interesting properties including high catalytic efficiency, catalyst support, and strong adsorption ability. Recently, ZnO has been considered as a promising material for biosensor applications because of its high isoelectric point (9.5), biocompatibility, and abundance in nature.[23] The high isoelectric point of ZnO results in a unique property to immobilize an enzyme having a low isoelectric point (4.7 ChOx) through electrostatic interaction. Furthermore, nontoxicity, high chemical stability, and high electron transfer capability make ZnO a favorable material for immobilization of biomolecules without an electron mediator and it can be employed for developing implantable biosensors.[22−25]

On the other hand, doping in ZnO with noble metals[26] offers an effective approach to enhance the properties of nanostructures, which is crucial for their practical applications. Besides many successful demonstrations, it remains a grand challenge to produce large quantities of one-dimensional ZnO nanostruc-

* Corresponding author. Fax: 86-10-62771160. E-mail: jzhu@mail.tsinghua.edu.cn.
[†] Department of Material Science and Engineering.
[‡] Department of Chemical Engineering.

10.1021/jp9089497
Published on Web 11/17/2009

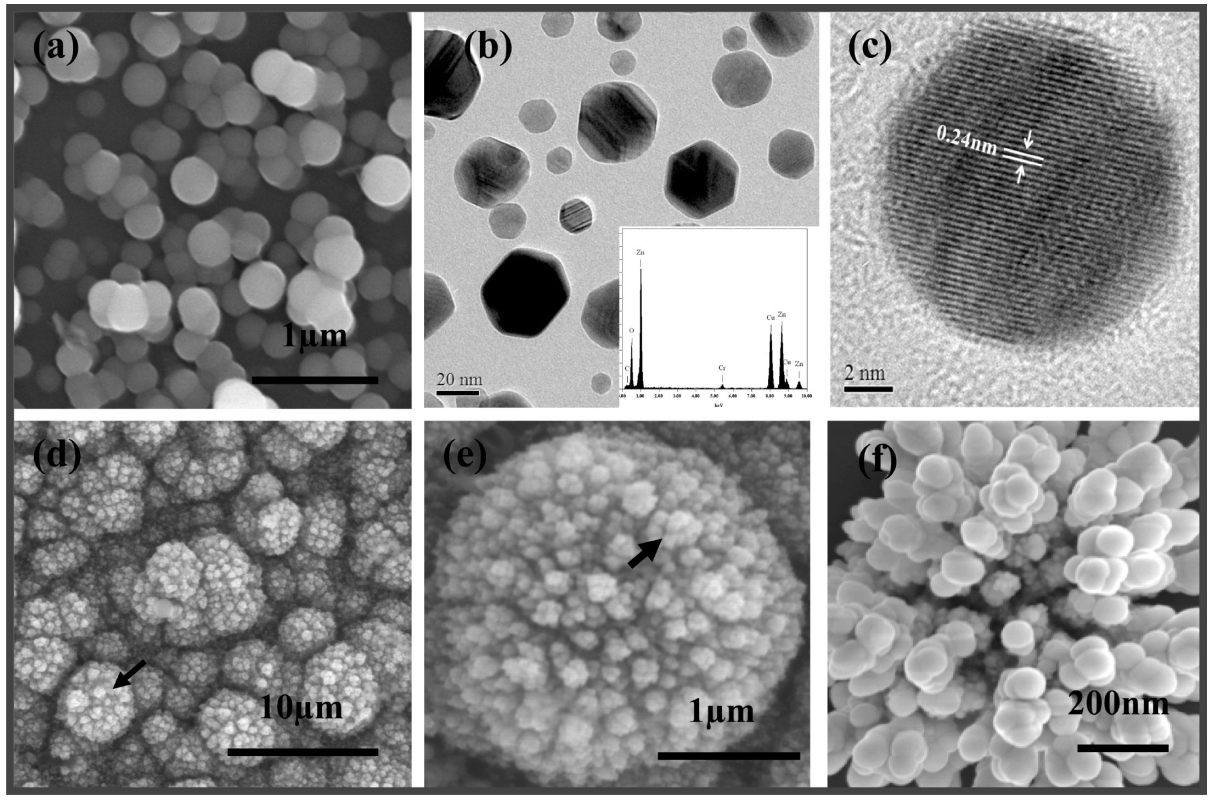

Figure 1. (a) SEM image of ZnO nanospheres. (b) TEM image along with EDS of ZnO nanospheres. (c) HRTEM image of individual ZnO nanosphere. (d−f) Typical SEM images of the as-deposited Pt-incorporated ZnO nanospheres. (d) Low-magnification image of spherical agglomerates of nanospheres. (e) Individual agglomerate sphere taken from the arrow point in (d). (f) Pt−ZnO nanospheres on the surface of self-assembled microspheres from the arrow point in (e).

ture doped with platinum, together with well-controlled dimensions and morphologies. The main focus of the present study is to construct a very highly sensitive cholesterol biosensor working at very low applied potential. To meet the desired requirements, Pt-incorporated fullerene-like ZnO nanospheres are synthesized by electrodeposition on a glassy carbon electrode. The electrocatalytic behavior of Pt−ZnO nanospheres (PtZONS) modified GCE toward the electrochemical oxidation of hydrogen peroxide and a Nafion/ChOx/PtZONS/GCE-based biosensor for the determination of cholesterol are investigated and discussed.

II. Experimental Section

II.1. Reagents. Cholesterol oxidase (EC 1.1.3.6, 28 U/mg) was purchased from Sigma-Aldrich (Shanghai) Trading Co., Ltd. Glucose, cholesterol, L-cysteine, ascorbic acid, and urea were purchased from Sinopharm Chemical Regent Co. Ltd. Hexachloroplatinic acid (99.998%) was supplied by Sigma-Aldrich. Hydrogen peroxide (30%) and 2-propanol (99.9%) were obtained from Beijing Modern Eastern Fine Chemical. Zinc nitrate hexahydrate ($ZnNO_3 \cdot 6H_2O$, 99%) and hexamethylenetetramine (HMTA, 99%) were also purchased from Sinopharm Chemical Reagent Co., Ltd., and Nafion (5 wt %) was purchased from Dupont. Other chemicals were of analytical-reagent grade without further purification. The cholesterol stock solution was prepared in a 50 mL aqueous solution containing 1 mL of 2-propanol and 1 mL of Triton X-100 in a bath at 60 °C and then diluted with deionized water. All solutions in the testing were prepared using deionized water.

II.2. Apparatus. The electrochemical experiments were performed at room temperature utilizing an electrochemical workstation (CHI660C) with a three-electrode configuration. A modified glassy carbon electrode (3 mm in diameter) was used as the working electrode, with Hg/Hg_2SO_4 as the reference electrode, and platinum as the counter electrode. The pH of the solution was measured with a KL-009(1) meter. The as-synthesized PtZONS were characterized by scanning electron microscopy (SEM-6301F), high-resolution transmission electron microscopy (HRTEM; JEM-2011), energy dispersive X-ray spectroscopy (EDS), and X-ray photospectroscopy (XPS).

II.3. Synthesis of ZnO and Pt−ZnO Nanospheres. For the synthesis of ZnO and PtZONS, a conventional GCE (with 3 mm in diameter) was used as the substrate electrode. PtZONS were electrochemically deposited with a simple electrochemical cell controlled by a CHI660C electrochemical workstation. The electrolyte was 100 mL of aqueous solution containing 0.01 M $ZnNO_3$, 0.01 M HMTA, and 0.01 M $H_2PtCl_6 \cdot (H_2O)_6$. The applied voltage was 1 V with a current density about 7.073 mA cm^{-2} at room temperature. After 1 h deposition, the PtZONS were obtained on the GCE surface. The ZnO nanospheres were also synthesized with the same conditions without 0.01 M $H_2PtCl_6 \cdot (H_2O)_6$. Before modification, the electrodes were washed successively in acetone, ethanol, and deionized water and dried at 60 °C for 2 h.

II.4. Cholesterol Biosensor Fabrication. Before the immobilization of ChOx, ZnO and PtZONS modified electrodes were rinsed with phosphate-buffered solution (PBS) to generate hydrophilic surfaces. The enzyme solution was prepared by dissolving ChOx (1.0 mg/mL) in 0.1 M (0.9% NaCl) phosphate-buffered saline (PBS, pH 6.8) for 24 h. A 5 μL volume of the above solution was immobilized onto the surface of as-prepared ZnO/GCE and PtZONS/GCE by physical adsorption. The modified electrodes were then left in air for 2 h to dry, which also allowed ChOx to absorb onto the ZnO and Pt−ZnO

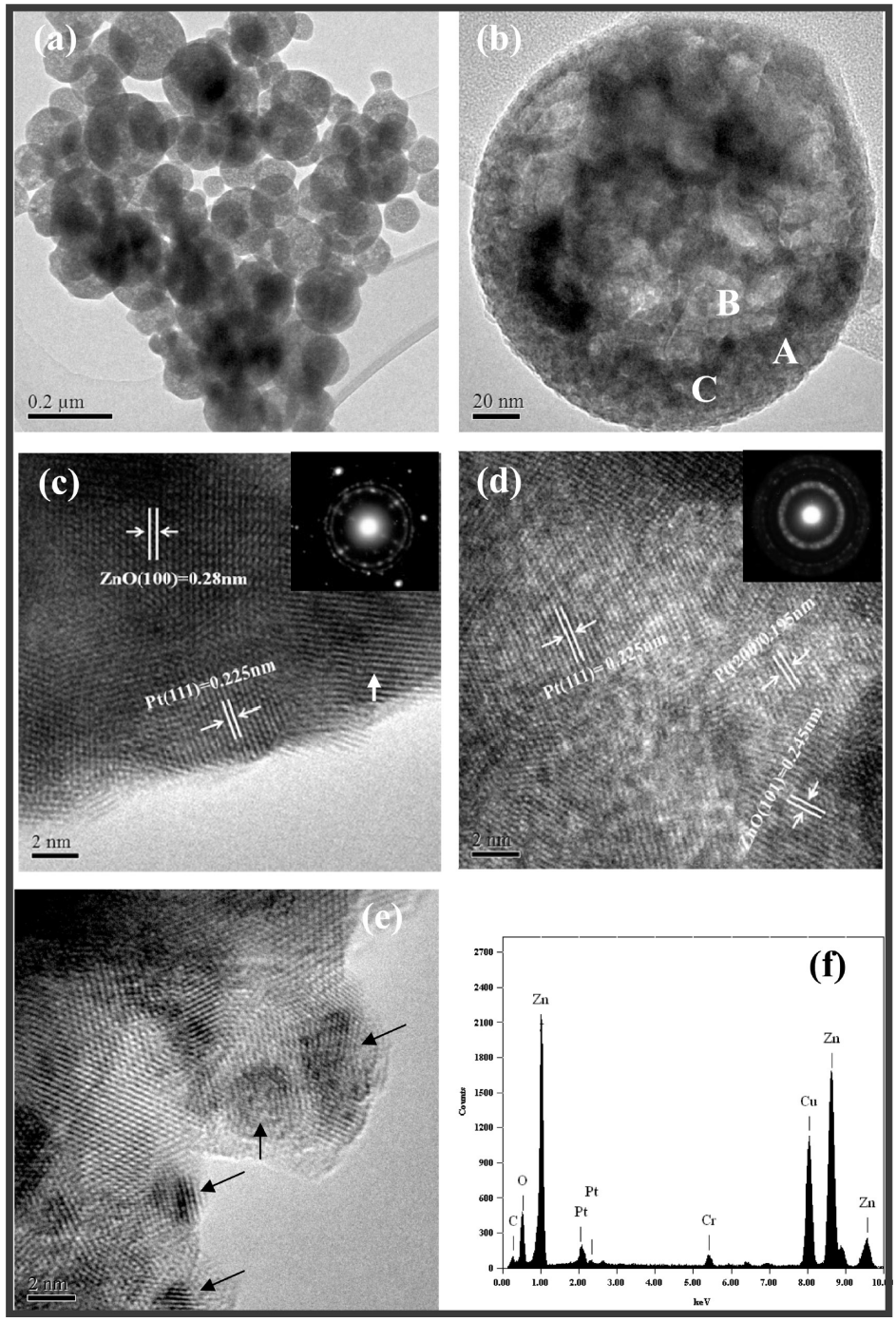

Figure 2. (a) Low-magnification TEM image of Pt−ZnO nanosphere agglomeration. (b) Magnified TEM image of individual Pt−ZnO nanosphere. (c−e) Bright field HRTEM images of the nanosphere from the indicated area (A, B, C) in (b); insets are SAED of the nanosphere. (f) EDS of Pt−ZnO nanospheres.

nanospheres. After drying at room temperature, 1 μL of 5 wt % Nafion solution was further dropped onto the electrode surfaces to prevent possible enzyme leakage and eliminate foreign interferences. Finally, the electrodes were immersed in deionized water to remove unimmobilized enzyme. The electrodes were stored in dry conditions at 4 °C when not in use.

III. Results and Discussion

III.1. Characterization of Pt−ZnO Nanospheres. SEM has been employed to analyze the microstructural characteristics of the as-deposited products. Figure 1a shows that the morphology of the product consisted of ZnO nanospheres with an average diameter in the range 10−200 nm. The TEM image of the ZnO nanospheres along with the EDS (inset) is shown in Figure 1b. The HRTEM image of a single ZnO nanosphere is shown in Figure 1c which demonstrates the single-crystalline nature. The interplanar distance of fringes is measured to be 0.24 nm, which corresponds to the spacing of (101) planes of wurtzite ZnO. Figure 1d shows that the overall morphology of the obtained product consisted of spherical agglomerates of PtZONS in a high density with an average diameter in the range 0.2−3.5 μm. A magnified SEM image of the single agglomerate taken from the arrow point is shown in Figure 1e and illustrates that the PtZONS assembled into many separate spherical agglomerates on the surface of the first spherical agglomerate as shown in Figure 2e. A close observation from Figure 1e reveals that

PtZONS have a fullerene-like spherical shape with diameters of about 50−200 nm as shown in Figure 1f. This demonstrates that the nanospheres could be assembled into spherical aggregates under electrodeposition and then serve as a substrate for further agglomeration.

In order to further investigate the microstructure of PtZONS three-dimensional assembly, TEM and HRTEM images have been recorded as shown in Figure 2a−e. The TEM image of self-assembled agglomerates and the magnified TEM image of an individual PtZONS are shown in Figure 2a,b. The HRTEM images taken from the points (A, B, C in Figure 2b) are shown in Figure 2c−e and indicate that the surfaces of nanospheres are uniform ripple-like edges which may appear due to the Pt incorporation. It is also observed that the nanosphere has a polycrystalline nature as shown in the figure. The interplanar distances of fringes are measured to be 0.28 and 0.24 nm, which correspond to the spacing of the (100) and (101) planes of wurtzite ZnO. The interplanar distances are also measured to be 0.225 and 0.195 nm, corresponding to the spacing of the (111) and (200) Pt planes as shown in Figure 2c,d. Selected area electron diffraction (SAED) over a dozen nanosphere is performed as shown in the insets of Figure 2c,d. The arrows in Figure 2e indicate the Pt nanoparticles incorporated into ZnO nanospheres.

The amount of Pt has been investigated through EDS elemental analysis. Figure 2f shows the EDS spectrum taken from point B indicated in Figure 2b. An oxygen peak at about 0.52 keV and Zn peaks at about 1.02, 8.67, and 9.60 keV can be observed in the spectra. The signals of Cu, C, and Cr peaks come from the surface of the copper grid used for TEM measurement. The Pt peaks also appear at about 2.12 keV, which confirms the presence of Pt nanoparticles in nanospheres. Quantitative analysis reveals that the average amount of Pt content is about 2 atom % in each Pt−ZnO nanosphere. Statistical analysis of EDS measurements over a dozen PtZONS demonstrates that the incorporated Pt nanoparticles are randomly distributed into the ZnO nanospheres. Thus EDS results further demonstrate that Pt is incorporated into ZnO, which is also in good agreement with the HRTEM results.

The valence state of the Pt element in PtZONS has been analyzed by XPS. The prepared sample shows that the Pt peaks are located at 70.3 and 73.6 eV corresponding to the electronic states of Pt $4f_{7/2}$ and Pt $4f_{5/2}$, respectively, as shown in Figure 3a. The energy difference between two peaks is about 3.3 eV, which is similar to the reported value.[27] These peaks confirm the presence of metallic platinum, and the smaller doublet at 75.6 eV (higher binding energy side) reveals the existence of a $Pt^{\delta+}$ state of this metal (e.g., formation of PtO_x on Pt), similar to the Au 4f assignment for surface oxide.[28] On the other hand, the XPS spectrum of Zn is shown in Figure 3b corresponding to Zn $2p_{3/2}$ and Zn $2p_{1/2}$ peaks. From the peak positions it is observed that the Pt binding energy peaks are slightly shifted toward the lower binding energy side while the Zn peaks shift toward the higher binding energy side with respect to the reported values.[27,29] These binding energy shifts are due to the Pt incorporation into ZnO nanospheres. Furthermore, an increase in neutral platinum content of the as-deposited PtZONS film is also observed which is similar to that reported previously for Pt:ZnO film.[26] It also suggests the successful Pt incorporation into ZnO lattice because the formation of the Pt−ZnO bond may involve a net charge transfer. Thus platinum is predicted to serve as a stable electron donor to the conduction band of ZnO. The average contents of Pt are consistent with the EDS measurements.

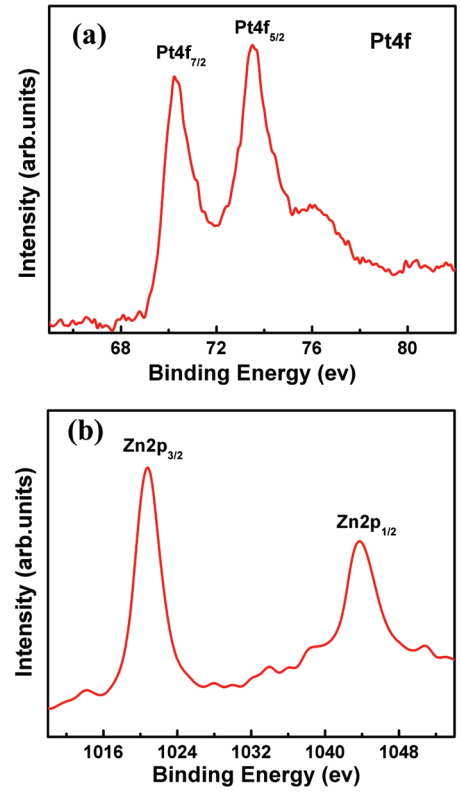

Figure 3. XPS analysis of (a) Pt 4f and (b) Zn 2p.

III.2. Detection of H_2O_2 with Pt−ZnO Modified Glassy Carbon Electrode. The enzymatic generation of hydrogen peroxide (eq 1) is achieved in the reaction layer of the PtZONS film. To investigate the electrocatalytic behavior toward the electrochemical reaction of hydrogen peroxide (eq 2) at the PtZONS film, the modified electrode is characterized by a cyclic voltammetric (CV) sweep curve ranging from −0.8 to +0.2 V versus Hg/Hg_2SO_4 at a scan rate of 50 mV/s. For comparison, a controlled experiment without the modified electrode was performed to record the background current response as seen CV a in Figure 4a. The CVs with PtZONS film modified GCE before and after addition of 10 μM H_2O_2 in 0.1 M phosphate buffer solution (pH 6.8) are shown in Figure 4a as CVs b and c. The two electrodes show only a small background current in the absence of hydrogen peroxide. Upon addition of hydrogen peroxide, the CV changed dramatically with obvious increases of the oxidation current in the range −0.1 to +0.2 V versus Hg/Hg_2SO_4 and the reduction current in the range −0.1 to −0.8 V at the PtZONS modified GCE as can be seen CV c (Figure 4a). This can be attributed to the incorporation of Pt nanoparticles in ZnO nanospheres which led to enhance the electrocatalytic ability and demonstrates that the electrodeposited PtZONS film allows the determination of cholesterol at a lower working potential.

The typical amperometric responses of the PtZONS modified GCE to the addition of varying concentrations of hydrogen peroxide at a working potential of +0.2 V versus Hg/Hg_2SO_4 are shown in Figure 4b. The modified electrode exhibits a rapid and sensitive response to the change of hydrogen peroxide concentration and an obvious increase in current upon successive addition of H_2O_2. The detection limit for the modified electrode toward H_2O_2 is 0.25 μM as shown in Figure 4c. The corresponding calibration plot shown in Figure 4d indicates the linear increase in response current upon the increase in H_2O_2 concentration with a linear range from 1.5 to 9 μM. All these results

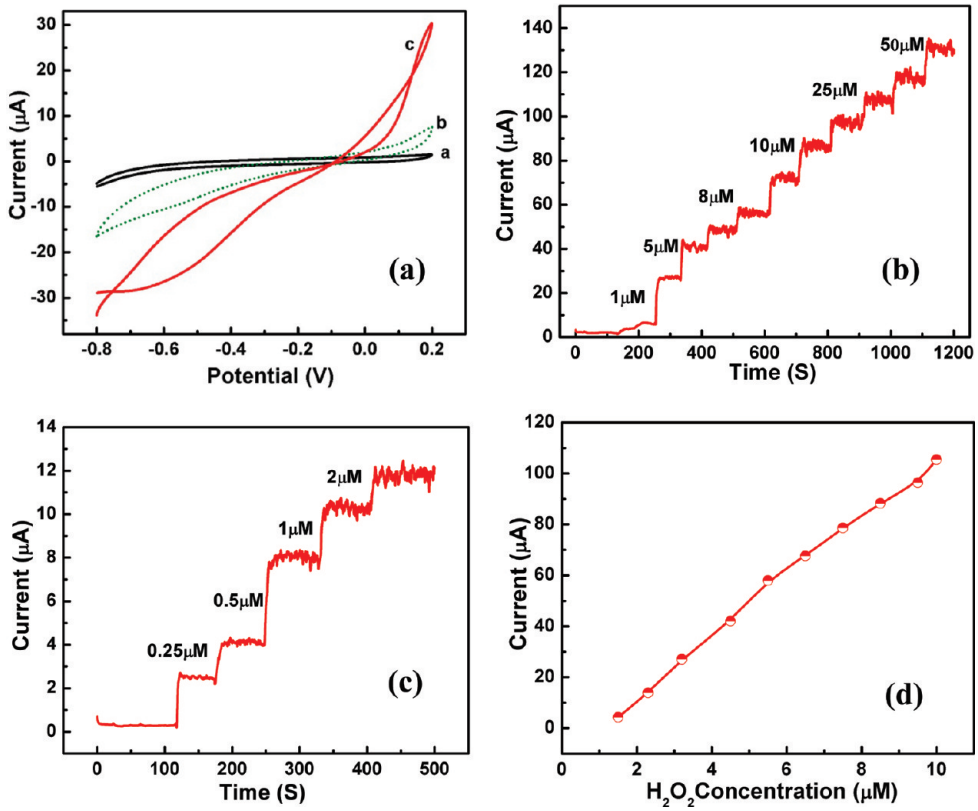

Figure 4. (a) Cyclic voltammograms of without modified GCE (CV a) and with modified GCE in the absence (CV b) and in the presence (CV c) of 5 μM H_2O_2 in pH 6.8 PB solution. (b) Amperometric response of modified electrode to different concentrations of hydrogen peroxide at +0.2 V in stirred pH 6.8 PB solution. (c) Amperometric response of modified GCE with successive increases in H_2O_2 concentration showing low limit of detection. (d) Calibrated curve of modified GCE with different concentrations of H_2O_2.

exhibit the electrocatalytic action of Pt incorporated nanoparticles in ZnO.

III.3. Determination of Cholesterol at Pt−ZnO Modified Glassy Carbon Electrode. ***III.3.1. Cyclic Voltammograms.*** A schematic of the modification of GCE with PtZONS, ChOx, and Nafion for efficient detection of cholesterol is shown in Figure 5a. The electrochemical measurements of the modified enzyme electrode have been investigated by cyclic voltammetric (CV) sweep curves in the range −0.8 to +0.2 V. Figure 5b exhibits the CV response of the Nafion/ChOx/PtZONS/GCE modified electrode in the absence (CV a) and in the presence (CV c) of 100 μM cholesterol at a scan rate of 50 mV/s. The CV response of the Nafion/ChOx/ZnO/GCE modified electrode in the presence of 100 μM cholesterol at a scan rate of 50 mV/s is also shown as curve b. The differences between the response currents for the three modified electrodes can be clearly observed from CVs a, b, and c. It can be seen that the electrochemical oxidation of the H_2O_2 released from the enzymatic reaction started at about 0.02 V (versus Hg/Hg_2SO_4) and continued until the potential reached +0.2 V in the presence of cholesterol. The CVs at different cholesterol concentrations (not shown) exhibited similar patterns, and higher cholesterol concentrations yielded larger oxidation currents as expected in the specific potential ranges mentioned above. This result shows that the incorporated Pt nanoparticles electrocatalyzed the oxidation of hydrogen peroxide and raised the response currents.

III.3.2. Current−Time Relationship for the Cholesterol Measurement in Solution. The performance of the biosensor has been investigated under different cholesterol concentration solutions. Figure 6a shows amperometric responses of the Nafion/ChOx/PtZONS/GCE and Nafion/ChOx/ZnO/GCE modified electrodes on the successive addition of cholesterol (from

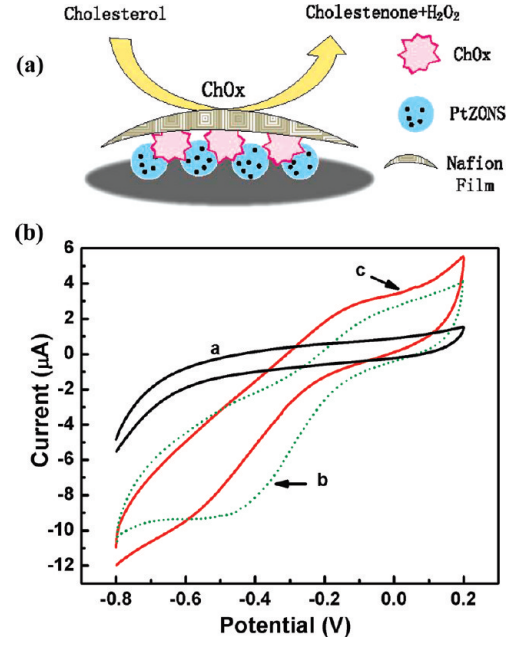

Figure 5. Schematic of modification of glassy carbon electrode with Pt-incorporated fullerene-like ZnO nanospheres, ChOx, and Nafion for efficient detection of cholesterol. (b) Cyclic voltammetric sweep curve of the Nafion/ChOx/PtZONS/GCE electrode in the absence (CV a) and in the presence (CV c) of 100 μM cholesterol in PB solution (pH 6.8) at a scan rate of 50 mV/s; CV curve of the Nafion/ChOx/ZnO/GCE electrode in the presence of 100 μM cholesterol (CV b) in PB solution (pH 6.8) at scan rate of 50 mV/s.

1 to 80 μM) into continuously stirred 0.1 M PB solution (pH 6.8) at an applied potential of +0.2 V. It has been revealed that

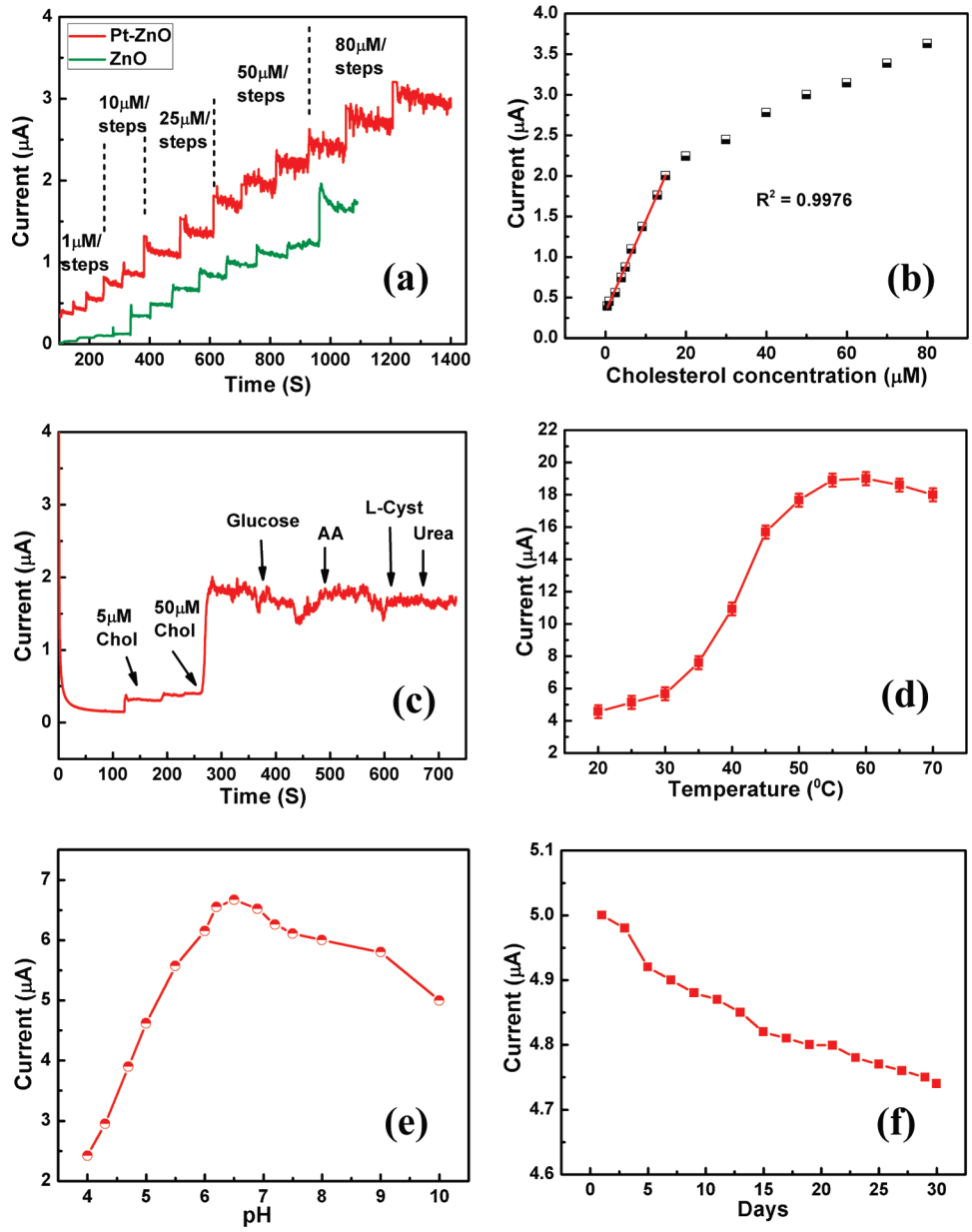

Figure 6. (a) Amperometric response of the biosensor based on ZnO and Pt−ZnO nanospheres to different cholesterol concentrations at +0.2 V in stirred pH 6.8 PB solutions. (b) Calibrated curve of the biosensor with successive additions of cholesterol. (c) Effect of interfering species on the response of the biosensor. (d) Temperature profile of the cholesterol biosensor in PB solution with 100 μM cholesterol. (e) Amperometric response of the biosensor in PB solution with increasing pH containing 50 μM cholesterol. (f) Long-term stability of the biosensor.

the biosensor based on PtZONS exhibits a rapid and sensitive response to the change of cholesterol concentration and an obvious increase in current upon successive addition of cholesterol. The modified electrode achieved 95% steady state current within less than 5 s. This indicates a good electrocatalytic oxidative and fast electron exchange behavior of the modified electrode. The difference between the amperometric responses of the two modified electrodes can be clearly observed in the figure. The corresponding calibration curve of the biosensor based on PtZONS is shown in Figure 6b. Following the increase of the cholesterol concentration, the response current increases and saturates at high concentration of cholesterol, which suggests the saturation of active sites of the enzyme at those cholesterol levels. The linear range of the calibration curve is from 0.5 to 15 μM (correction coefficient $R = 0.9976$). The sensitivity of the PtZONS based biosensor is about 1886.4 mA M^{-1} cm^{-2}, which is much higher than the immobilization matrix using MWCNT−CHIT−Pt composite thin film (44 mA M^{-1} cm^{-2}),[30] poly(2-hydroxyethyl methacrylate)−polypyrrole composite film (19.05 μA M^{-1} cm^{-2}),[31] polypyrrole (622.2 μA M^{-1} cm^{-2}),[32] polyaniline (2217.8 μA M^{-1} cm^{-2}),[33] ZnO nanoporous thin film (3.01 mA M^{-1} cm^{-2}),[34,35] and poly(pyrrole-*co*-*N*-methylpyrrole) film (0.6406 mA M^{-1} cm^{-2}).[36] To the best of our knowledge, this is the first time such a very high sensitivity at very low potential has been achieved for a cholesterol biosensor by using Nafion/ChOx/PtZONS/GCE modified electrode. These results prove that PtZONS used as the matrix increases the enzyme activity, which in turn enhances the sensitivity of the modified electrode to cholesterol detection.

III.3.3. Anti-interference Ability of Pt−ZnO Modified Glassy Carbon Electrode. It is well-known that some electroactive species in serum may influence the performance of a biosensor; therefore, the anti-interference ability of the biosensor is investigated by introducing electroactive species such as glucose, ascorbic acid (AA), L-cysteine (L-Cys), and urea. These species are consecutively added into continuously stirred 0.1 M PB

TABLE 1: Comparison of the Responses of Some Cholesterol Biosensors Constructed Based on Different Modified Materials

electrode materials	sensitivity/mA M^{-1} cm^{-2}	linear range/μM	response time/s	applied potential/V	ref
MWCNT−CHIT−Pt	44	5−30	8	0.4	30
poly(2-hydroxyethyl methacrylate)−polypyrrole	19.05×10^{-3}	−	30	−	31
polypyrrole	43.99×10^{-3}	$(0.025-0.3) \times 10^3$		0.7	32
polyaniline	2217.8×10^{-3}			0.45	33
ZnO nanoporous thin film	3.01	$(1.1-4.83) \times 10^3$		0.9	35
poly(pyrrole-*co*-*N*-methyl pyrrole)	0.6406		19	1.2	36
Pt−ZnO	1886.4	0.5−15	<5	0.2	present work

solution (pH 6.8) at an applied potential of +0.2 V with a scan rate of 50 mV/s. The influence of the above species on the detection of cholesterol at the modified electrode is shown in Figure 6c. It is observed that glucose and L-cysteine have no obvious effect on the biosensor, while ascorbic acid can cause a small current increment of about 5% compared with 50 μM cholesterol. However, a decrease in current of about 3% is also observed when 0.5 M urea is added. These results indicate that the proposed cholesterol biosensor exhibited the ability to reduce the influence of possible interferences. All the above results demonstrate that the combination of ZnO and Pt nanoparticles facilitates the low potential amperometric detection of cholesterol and enhances the anti-interference ability of the biosensor.

III.3.4. Thermal Stability of the Biosensor. Enzyme or proteins are susceptible to thermal denaturation; however, when they are immobilized onto a conducting surface, their thermal behavior will differ from that when they are in the "free" state.[37] The effect of varying temperature on the biosensor response with 100 μM cholesterol is also examined between 20 and 70 °C. As illustrated in Figure 6d, the current response gradually increases with the increasing temperature and reaches its optimum value at 55 °C. This is because the enzyme activity increases at higher temperature. After 55 °C the response decreases, which is caused by the natural thermal degradation of the enzyme. The hydrophobic PtZONS provided a favorable environment for the immobilized ChOx, which greatly enhanced the thermal stability of the biosensor. This suggests that the biosensor could be used in the environment within a temperature range of 20−55 °C. Although the biosensor shows a maximum response at 55 °C, all the experiments are done at room temperature (25 °C) to prevent possible solution evaporation and ease of operations.

III.3.5. pH Effect. The activity of the enzyme ChOx is much affected by the pH of the cholesterol solution; therefore, the pH effect on the biosensor performance is also investigated by measuring the current response to 100 μM cholesterol at +0.2 V. As the ZnO is a kind of amphoteric compound and is not stable in both strong acid and base solutions, the pH dependence of the biosensor is evaluated in the range of pH 4−10 in this experiment. As clearly seen in Figure 6e, the biosensor shows an optimal sensitivity of response at pH range 6.0−7.5 corresponding to a series of pH values. Considering that the pH of human blood is about 7.4, all the amperometric experiments have been carried out at pH 6.8.

III.3.6. Long-Term Stability. The long-term stability of the biosensor is also evaluated by measuring its performance after every few days as shown in Figure 6f. It can be seen that the biosensor shows high stability for cholesterol detection, which retains about 95% of its original response to cholesterol after 30 days of storage. The small decrease in cholesterol response may be due to the loss of the bioactivity of the immobilized ChOx with the passage of time.

III.3.7. Performance Comparison. The characteristics and performance of the fabricated biosensor are compared with those of previously reported cholesterol biosensors based on the utilization of various materials as the working electrode as shown in the Table 1. It is confirmed that the presented cholesterol biosensor exhibited an excellent performance.

IV. Conclusions

In conclusion, a highly sensitive cholesterol biosensor has been successfully fabricated by modifying a glassy carbon electrode with electrodeposited Pt-incorporated fullerene-like ZnO nanospheres. A highly reproducible sensitivity of 1886.4 mA M^{-1} cm^{-2}, a response time less than 5 s, and a linear range of 0.5−15 μM has been found from the fabricated biosensor. It has been found that the combination of ZnO and Pt nanoparticles (PtZONS) facilitates the low potential amperometric detection of cholesterol and enhances the anti-interference ability of the biosensor. Furthermore, it has been revealed that ZnO improves the electrocatalytic activity of Pt nanoparticles, which in turn enhances the sensitivity of the biosensor for cholesterol detection. Importantly, to the best of our knowledge, this is the first time such a very high sensitivity at very low potential has been achieved for a cholesterol biosensor by using a Nafion/ChOx/PtZONS/GCE modified electrode. Hence, PtZONS provide a new platform for biosensor design and other biological applications.

Acknowledgment. This work is financially supported by National 973 Project of China and the Chinese National Nature Science Foundation.

References and Notes

(1) Nauck, M.; Marz, W.; Weiland, H. *Clin. Chem.* **2000**, *46*, 436.
(2) Laboratory Standardization Panel of the National Cholesterol Education Program. *Clin. Chem.* **1988**, *34*, 193.
(3) Zak, B. *Am. J. Clin. Pathol.* **1957**, *27*, 583.
(4) Karube, I.; Hara, K.; Matsuoka, H.; Suzuki, S. *Anal. Chim. Acta* **1982**, *139*, 127.
(5) Yamato, H.; Koshiba, T.; Ohwa, M.; Wernet, W.; Matsumura, M. *Synth. Met.* **1997**, *87*, 231.
(6) Arjsiriwat, S.; Tanticharoen, M.; Kirtikara, K.; Aoki, K.; Somasundrum, M. *Electrochem. Commun.* **2000**, *2*, 441.
(7) Huang, H.; Yuan, Q.; Yang, X. *Colloid Surf., B: Biointerfaces* **2004**, *39*, 31.
(8) Hrapovic, S.; Liu, Y.; Male, K. B.; Luong, J. H. T. *Anal. Chem.* **2004**, *76*, 1083.
(9) Ren, X.; Meng, X.; Tang, F. *Sens. Actuators, B: Chem.* **2005**, *110*, 358.
(10) Becerik, I.; Kadirgan, F. *J. Electroanal. Chem.* **1989**, *436*, 189.
(11) Vidal, J. C.; Garcia-Ruiz, E.; Castillo, J. R. *J. Pharm. Biomed. Anal.* **2000**, *24*, 51.
(12) Dominguez Sanchez, P.; Tuñón Blanco, P.; Fernandez Alvarez, J. M.; Smyth, M. R.; O'Kennedy, R. *Electroanalysis* **1990**, *2*, 303.
(13) Hendji, A. N.; Bataillard, P.; Jaffrezic-Renault, N. *Sens. Actuators, B: Chem.* **1993**, *15*, 127.
(14) Hall, S. B.; Khudaish, E. A.; Hart, A. L. *Electrochim. Acta* **2000**, *45*, 3573.
(15) Jagdish, C.; Pearton, S. J. *Zinc Oxide Bulk, Thin Flms and Nanostructures*; Elsevier: Oxford, U.K., 2006; p 600.
(16) Xiao, Y.; Patolsky, F.; Katz, E.; Hainfeld, J. F.; Willner, I. *Science* **2003**, *299*, 1877.

(17) Jia, J.; Wang, B.; Wu, A.; Cheng, G.; Li, Z.; Dong, S. A. *Anal. Chem.* **2002**, *74*, 2217.
(18) Xua, Q.; Mao, C.; Liu, N. N.; Zhu, J. J.; Sheng, J. *Biosens. Bioelectron.* **2006**, *22*, 768.
(19) Zhu, X.; Yuri, I.; Gan, X.; Suzuki, I.; Li, G. *Biosens. Bioelectron.* **2007**, *8*, 1600.
(20) Fan, Z. Y.; Lu, J. G. *Appl. Phys. Lett.* **2005**, *86*, 123510.
(21) Xu, C. X.; Sun, X. W.; Yuen, C. B.; Chen, J.; Yu, S. F.; Dong, Z. L. *Appl. Phys. Lett.* **2005**, *86*, 011118.
(22) Kumar, S.; Gupta, V.; Sreenivas, K. *Nanotechnology* **2006**, *16*, 1167.
(23) Wang, J. X.; Sun, X. W.; Wei, A.; Lei, Y.; Cai, X. P.; Li, C. M.; Dong, Z. L. *Appl. Phys. Lett.* **2006**, *88*, 233106.
(24) Krishnamurthy, S.; Bei, T.; Zoumakis, E.; Chrousos, G. P.; Iliadis, A. *Biosens. Bioelectron.* **2006**, *22*, 707.
(25) Wei, A.; Sun, X. W.; Wang, J. X.; Lei, Y.; Cai, X. P.; Li, C. M.; Dong, Z. L.; Huang, W. *Appl. Phys. Lett.* **2006**, *89*, 123902.
(26) Gregory, J. E.; Aimee, R.; Li, Q. W.; Charles, F. W., Jr. *J. Vac. Sci. Technol., A* **1998**, *16*, 1926.
(27) Yao, K. X.; Zeng, H. C. *Langmuir* **2008**, *24*, 14234.
(28) Zhang, Y. X.; Zeng, H. C. *J. Phys. Chem. C* **2007**, *111*, 6970.
(29) Christina, B.; Chantal, P.; Martin, C.; Gianluigi, A. B.; Barry, R. M. *J. Am. Chem. Soc.* **2004**, *126*, 8028.
(30) Yu, C. T.; Siao, Y. C.; Chen, A. L. *Sens. Actuators, B: Chem.* **2008**, *135*, 96.
(31) Brahim, S.; Narinesingh, D.; Guiseppi-Elie, A. *Anal. Chim. Acta* **2001**, *448*, 27.
(32) Vidal, J. C.; Garcia, E.; Castillo, J. R. *Anal. Chim. Acta* **1999**, *385*, 213.
(33) Wang, H.; Mu, S. *Anal. Chim. Acta* **1999**, *379*, 193.
(34) Singh, S. P.; Sunil, K. A.; Pratibha, P.; Malhotra, B. D.; Shibu, S.; Sreeniivas, K.; Vinay, G. *Appl. Phys. Lett.* **2007**, *91*, 063901.
(35) Chia, Y. L.; Kuo, C. H. *AIP Conf. Proc.* **2009**, *1137*, 123.
(36) Singh, K.; Basu, T.; Pratima, R. S.; Bansi, D. M. *J. Mater. Sci.* **2009**, *44*, 954.
(37) Weetall, H. H. *Anal. Chem.* **1974**, *46*, 602A.

JP9089497